Recent modeling for the ITER ion cyclotron range of frequency antennas with the TOPICA code

PAPER • OPEN ACCESS

Recent modeling for the ITER ion cyclotron range of frequency antennas with the TOPICA code

To cite this article: D. Milanesio *et al* 2023 *Nucl. Fusion* **63** 046010

OPEN ACCESS
IOP Publishing | International Atomic Energy Agency
Nuclear Fusion
Nucl. Fusion **63** (2023) 046010 (11pp)
https://doi.org/10.1088/1741-4326/acb785

Recent modeling for the ITER ion cyclotron range of frequency antennas with the TOPICA code

D. Milanesio[1,*], W. Helou[2], V. Polli[2,3], F. Durodié[4], P. Lamalle[2], V. Maquet[4], A. Messiaen[4], W. Tierens[5] and W. Zhang[5,6]

[1] Dipartimento di Elettronica, Politecnico di Torino, Torino, Italy
[2] ITER Organization, Route de Vinon-sur-Verdon, CS 90 046, 13067 St. Paul Lez Durance Cedex, France
[3] Capgemini Engineering | France, Parc du Golf—Bat.17, 350 Av JRG Gautier de la Lauziere, CS40514, 13593 Aix en Provence Cedex 3, France
[4] LPP-ERM/KMS, TEC Partner, Brussels, Belgium
[5] Max-Planck-Institut für Plasmaphysik, Boltzmannstr. 2, 85748 Garching, Germany
[6] Institute of Plasma Physics, Chinese Academy of Sciences, Hefei, 230031, People's Republic of China

E-mail: daniele.milanesio@polito.it

Received 9 November 2022, revised 16 January 2023
Accepted for publication 31 January 2023
Published 1 March 2023

Abstract

This paper documents the analysis of the ITER ion cyclotron resonance heating (ICRF) launcher using the TOPICA code, throughout recent years' design activities. The ability to simulate the detailed geometry of an ICRF antenna in front of a realistic plasma and to obtain the antenna input parameters, the electric currents on conductors and the radiated field distribution next to the antenna is of significant importance to evaluate and predict the overall system performances. Starting from a reference geometry, we first investigated the impact of some geometrical and numerical factors, such as the Faraday Screen geometry or the mesh quality. Then a final geometry was the object of a comprehensive analysis, varying the working frequency, the plasma conditions and the poloidal and toroidal phasings between the feeding lines. The performance of the antenna has been documented in terms of input parameters, power coupled to plasma and electric fields. Eventually, the four-port junction has also been included in TOPICA models.

Keywords: ITER, ICRF antenna, ICRF heating, TOPICA

(Some figures may appear in colour only in the online journal)

1. Introduction

Ion cyclotron resonance heating (ICRF) is going to be one of the auxiliary heating systems in ITER [1]. In this respect, the capability to accurately predict the IC antenna behavior in terms of input parameters, power coupled to plasma, electric currents and radiated fields is crucial to assist its design. This paper contains an accurate analysis of the antenna performance in the expected working frequency range (from 35 MH to 60 MHz) given several different loading conditions, with the help of the TOPICA code. Several additional tests are also discussed, to better explore TOPICA's limitations and to understand the impact of some mechanical elements on the electromagnetic properties of the launcher. Sections 1.1–1.3 provide an overall description of the TOPICA code, of the simulated geometries and of the loaded plasma profiles, respectively. Section 2 describes a few preliminary tests, while

* Author to whom any correspondence should be addressed.

section 3 documents the analysis of the final geometry. Eventually, section 4 provides an insight into the impact of the four-port junction (4PJ) used to group poloidal triplets. It is important to stress here that this paper documents most of the TOPICA related actions for the analysis of the ITER IC launcher. However, being part of a wider cooperative design task, this paper has to be considered in synergy with the other published material on the same topic. In particular, interested readers can refer to [2–4] for the COMSOL and Petra-M modeling of the ITER ICRF antennas and the excellent agreement with the TOPICA results. Also [5, 6], analyze the fields extracted from the TOPICA simulations (near fields in front of the antenna, and fields inside the antenna plug/port cavity, respectively).

1.1. TOPICA code

All the results shown here have been obtained using the TOPICA code. In order to better understand the peculiarities of this design tool, a few words are required as a preamble. We refer the interested reader to [7, 8] for a more detailed description of the code.

TOPICA is a tool intended for the 3D/1D simulation of ICRF, i.e. accounting for antennas in a realistic 3D geometry and with an accurate 1D plasma model. The approach to the problem is based on an integral-equation formulation for the self-consistent evaluation of the current distribution on conductors. The environment is subdivided into two coupled regions: the plasma region and the vacuum region, in which the antenna is located. The two problems are linked by means of electromagnetic current distribution on the interface between the two regions, often referred to as *aperture*. In the vacuum region, all the calculations are executed in the spatial domain while in the plasma region calculations are executed in the spectral domain, which enables the use of a hot plasma model. The plasma enters the formalism via a surface impedance matrix; for this reason, any plasma model can be used. At present, a modified version of the hot plasma code FELICE is adopted [9], that affords density and temperature profiles, and finite Larmor radius effects. The source term directly models the TEM mode of the coax feeding the antenna and the current in the coax is determined self-consistently, giving the way to accurately compute the antenna input parameters.

From the functional point of view, the TOPICA code is fully parallelized. This feature leads not only to a remarkable saving in terms of computation time but also to the removal of any limitation on the complexity of the simulated geometries. TOPICA is currently installed on MARCONI cluster at CINECA (www.hcp.cineca.it), characterized by 3188 computing nodes, featuring Intel Xeon Skylake (SKL) processors and capable of a total peak performance of about 20 PFlop s^{-1}.

1.2. List of geometries

In terms of geometrical description, all simulated models share the same approach, i.e. the full array of 24 straps is enclosed within a cavity, as required by TOPICA's formulation, including a portion of the input transmission lines and, if available, a Faraday screen (FS). In order to provide an even more precise description of the antenna behavior, a part of the blanket shielding modules (BSMs) and the 4PJ are also included in some models. It is important to stress that the geometries simulated within this design activity are by far the largest, both geometrically and in terms of number of mesh unknowns, that have ever been analyzed with this numerical tool.

The first geometry to be simulated was the preliminary design review (PDR) antenna from 2010 (labeled here as 'CY8a'). This was the final geometry coming out of the first design phase [10, 11] and it was a top-bottom asymmetric launcher characterized by a curved antenna-plasma interface (i.e. *aperture*) and by a simplified FS. 'CY8a' aperture mimics the last plasma closed surface, which is located at a varying distance from the straps depending on the toroidal and poloidal position. This model was originally simulated on the HELIOS cluster at IFERC-CSC (www.iferc.org) with two groups of plasma profiles provided by ITER Organization, namely a low and a high density one; please see section 1.3 for their detailed description. A couple of runs have been repeated on the current cluster in use, i.e. MARCONI, to demonstrate their reproducibility. Figure 1 shows the entire launcher with a detailed view of the straps.

A second version of this antenna, characterized by a new curved aperture and by central symmetry (the full array is built mirroring one quarter of 'CY8a'), namely 'CY8b', was also simulated and was intended as the reference antenna for the next 'CY9' model. This new curved aperture is not related to equilibrium studies and it better follows the antenna front face, being top/bottom and left/right symmetric too; in other words, the strap-aperture distance varies less than in the 'CY8a' geometry, even if it is on average more distant from it. This increased strap-aperture distance automatically translates into worse coupled power of 'CY8b' launcher with respect to 'CY8a' one. Table 1 shows the precise range of distances between the straps and the plasma edge. The complete description of the ITER IC antenna performances through the entire design activity will be detailed in a devoted paper.

The next group of geometries was characterized again by central symmetry, by the new 'CY8b' aperture and, above all, by a reduced distance between the straps in the toroidal direction and by different strap short circuits shapes. These last features were the consequence of the mechanical review of the PDR antenna. The effect of the FS was also tested, first by completely removing it (model 'CY9b') and then by including a more realistic one (model 'CY9c') with respect to the simplified FS of model 'CY9a'. Results are displayed in section 2.2, while figure 2 details the FS shape inserted in geometries 'CY9a' and 'CY9c'.

Geometry 'CY9a' was also adopted to perform a sensitivity analysis of the mesh resolution on the aperture, as described in section 2.1. Keeping constant all geometrical features and the mesh resolution on conductors, the number of unknowns adopted to discretize the antenna-plasma interface was increased from 2550 to 5124 in four steps. In terms of size of the triangular mesh elements, the minimum size was increased from 49 to 68 mm, the maximum from 74 to 98 mm. It is important to stress that the maximum number of unknowns on the

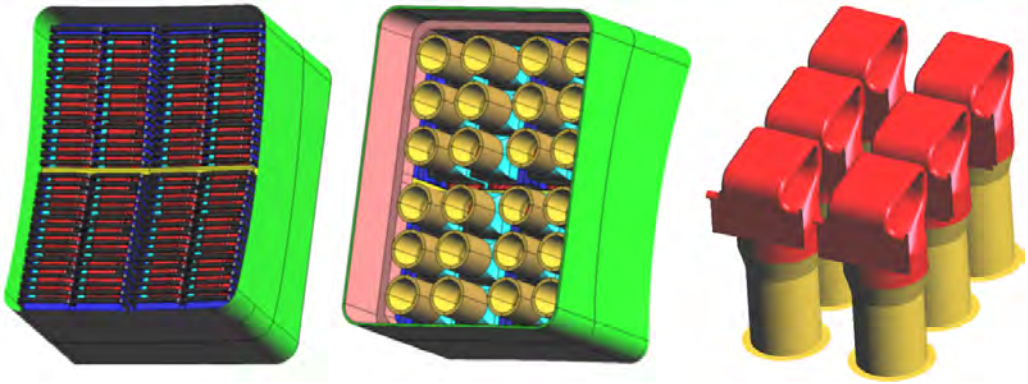

Figure 1. 2010 'CY8a' PDR reference launcher with a detailed view of the straps shape (right).

Table 1. Most relevant simulated geometries.

Geometry label	CY8a	CY8b	CY9(a/b/c)	CY10	CY11
Motivation	2010 PDR	Reference	Impact of mesh, FS, strap inter spaces modification and the strap short circuit shapes	Final model and impact of stretching procedure	Impact of 4PJ
Strap-plasma distance	40÷94 mm	78÷98 mm	78÷98 mm	65÷110 mm	as CY10
FS description	2010 PDR	Simplified	Different versions (also no FS)	Simplified	as CY10
Left-right symmetry	Yes	Yes	Yes	Yes	Yes
Top-bottom symmetry	top:6.76° bottom:4.78°	Yes (6.76°)	Yes	as CY8b	as CY8b
Total unknowns	172 k	181 k	145 k÷267 k	263 k	277 k
Unknowns on aperture	3552	4552	2550÷5124	4720	as CY10
Mesh max size on conductors	8.5 cm	8 cm	5 cm	8 cm	as CY10
Mesh max size on aperture	9.2 cm	7.4 cm	7.4÷9.8 cm	8.0 cm	as CY10
Mesh min size on aperture	6.0 cm	5.1 cm	5.1÷6.8 cm	5.6 cm	as CY10

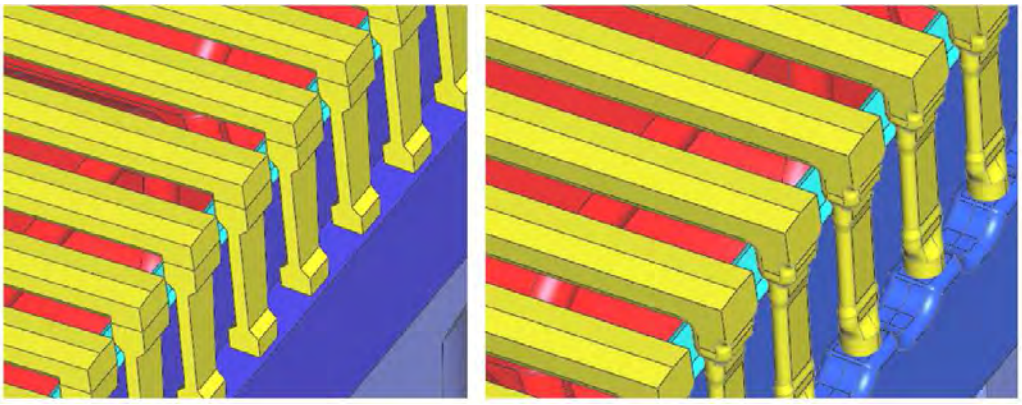

Figure 2. Simplified FS ('CY9a', on the left) vs. realistic FS ('CY9c', on the right).

aperture is bounded by the memory per node available on the computing cluster and, hence, cannot be raised at will.

The following geometry, namely 'CY10', corresponds to the latest antenna. It is characterized by a top-bottom asymmetry and by a poloidally and toroidally dependent strap-aperture distance, again derived by updated plasma equilibrium computations. The TOPICA model also includes a portion of the BSM all around the launcher, as the reader can notice from figure 3. Section 3 describes the performances of this antenna with a large number of plasma profiles for five frequency points; please refer to section 1.3 for the accurate description of the adopted loadings.

Eventually, the 4PJ was also included in TOPICA modeling. Geometry 'CY11' is identical to the previous 'CY10',

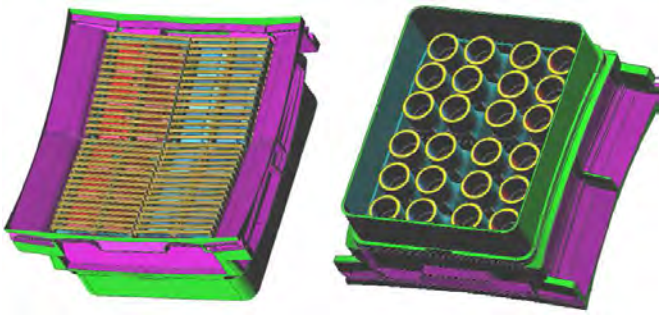

Figure 3. Front and back view of the 'CY10' launcher.

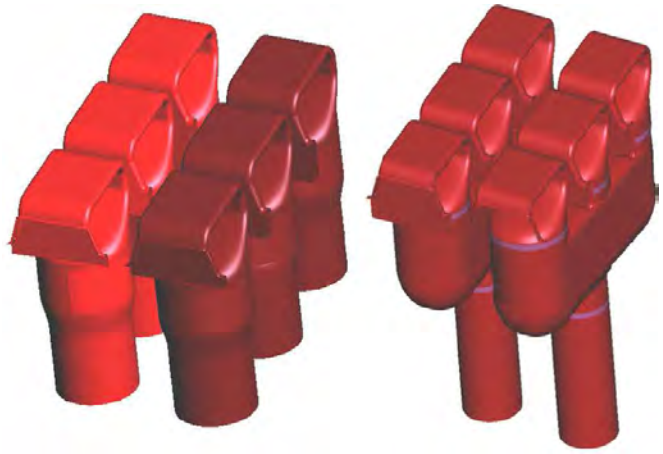

Figure 4. 'CY10' straps (left) vs. 'CY11' 4PJ (right).

with the addition of the 4PJ to group poloidal straps in triplets; figure 4 visually compares the single straps to the poloidal triplets, while section 3.1 documents the obtained results.

Table 1 summarizes some relevant features of the most important geometries listed before.

1.3. List of plasma profiles

Before proceeding with the description of all plasma cases, it is essential to recall how a plasma profile is handled by TOPICA. First of all, the part of the profile that enters the antenna cavity (i.e. that lies beyond the previously mentioned aperture) has to be immediately neglected, that region being in vacuum. A further action is then performed to take care of the S = 0 resonance (lower hybrid resonance), which is not correctly handled by FELICE code; the lower hybrid resonance [12] depends on several plasma parameters (plasma composition, density, magnetic field, etc) and it does not always appear in all profiles. The portion of the profile where the resonance is located is usually removed and substituted with an 'equivalent' layer of vacuum of the same thickness, hence keeping constant the separatrix-antenna distance. The amount of equivalent vacuum can reach a maximum of about 14 cm, but it is on average of the order of few centimeters and it is not needed in approximately 25% of the simulated plasma cases. Forcing the density to a constant value other than zero at the very plasma edge is an alternative approach. Figure 5(*A*) shows how the low density part of a plasma profile is modified according to the above mentioned solutions to handle S = 0 resonance, while (*B*) documents the behavior of S parameter absolute value as a function of the major radius for that profile (the antenna is located on the right). Figure 5(*C*) depicts the power coupled to plasma predicted by ANTITER II code (see appendices in [11]) as a function of the different solutions adopted in (*A*) and for a few toroidal input phasings, imposing 41 kV to the straps; it is important to stress that ANTITER II is implemented such as to be able to handle the LH resonance and the full profile case is also taken into account and added to the plot. (*C*) proves that the 'equivalent vacuum' choice ('hyp3' in the plot) can be considered a conservative approach in terms of power coupled to plasma. (*D*) shows that the same behavior of the coupled power as a function of the solution adopted in (*A*) is retrieved for TOPICA code as well. Then, by adding the conclusions derived in (*C*), one can state that the 'equivalent vacuum' approach is the most conservative choice that can be implemented in TOPICA to handle S = 0 resonance among the considered hypotheses (about 5%–10% less power with respect to the full profile case). In TOPICA, a 45 kV peak voltage along the strap triplets feeding lines is imposed, which corresponds to about 41 kV of voltage at the straps, i.e. where the feeding points are located in ANTITER II.

The equivalence theorem adopted in TOPICA formulation determines the presence of an infinitely extending ground plane at the aperture position, which reproduces the effect of the first wall (FW). Profiles can also be rigidly shifted in the radial direction to assess the impact on the antenna input parameters and on the transferred power. When moving the profile toward the antenna, the rigid shift is obtained by removing the low density part of it. Given the TOPICA formulation, this approach is considerably faster than assuming a constant aperture-FW position and moving the antenna radially, because only the interaction with plasma has to be recomputed. Conversely, when moving the profile away from the antenna, few centimeters from the low field side are added without removing any central density; this is allowed since no reflected power is assumed after 50 cm from the antenna mouth. Please notice that a negative shift is considered from the antenna perspective, i.e. corresponds to the plasma profile getting closer to the antenna itself.

Two reference plasma profiles were originally defined by ITER IO in 2010 and are depicted in figure 6 (plasma composition: 50% D, 50% T, magnetic field at center: 5.3 T); they represented the extremes within which the ITER plasmas were expected, given the uncertainties on edge physics [13]. Radial shifts of 2, 4 and 5 cm toward the antenna were considered for the low density profile, while the high density one was loaded only after a 4 cm shift away from the antenna.

Ten additional plasma profiles [14] were then provided by ITER IO in 2020, namely Case1 (low far SOL density LO and high far SOL density HI, about 56% D and 44% T, 5.4 T), Case2 (LO and HI, about 48% He4 and 4% H, 2.7 T), Case3 (LO and HI, about 51% D and 49% T, 5.4 T), Case4 (LO and HI, about 52% D and 48% T, 5.4 T) and Case5 (LO and HI, about 48% He4 and 4% H, 2.7 T). Radial shifts of 2, 4 and 5 cm

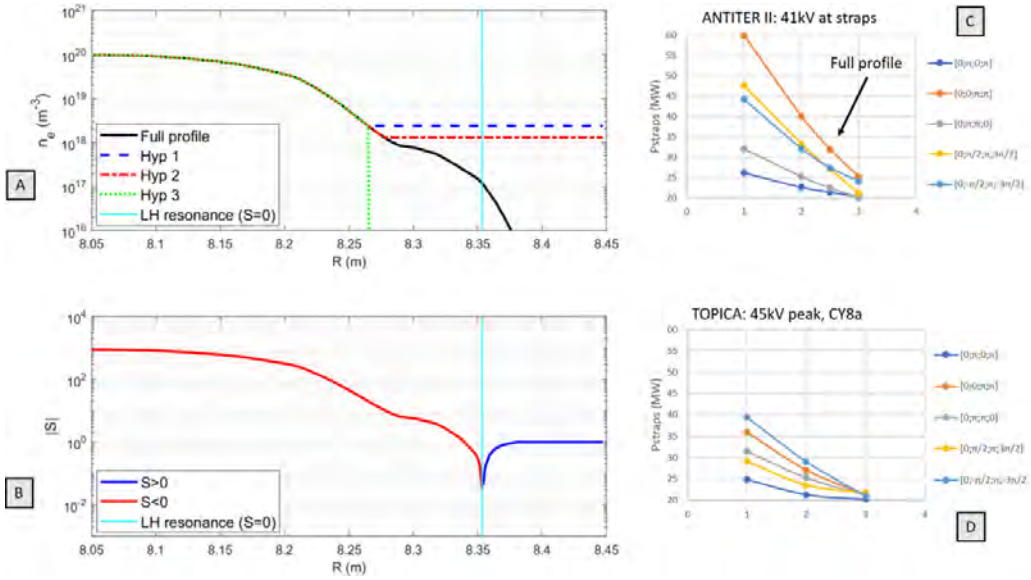

Figure 5. (*A*) The 2010 low density profile is plotted with three different approximations: in 'Hyp1' and 'Hyp2' the edge density is replaced with a constant density starting from S $= -20$ and S $= -10$ respectively, in 'Hyp3' the edge density is replaced by a vacuum layer starting from S $= -20$. (*B*) Absolute value of Stix parameters S is plotted. (*C*) Power coupled to plasma computed with ANTITER II at 55 MHz assuming 41 kV at the straps, for different input phasings; the full profile option is indicated directly on the graph. (*D*) Power coupled to plasma computed with TOPICA at 55 MHz for 45 kV peak voltage along the vacuum feeding lines for different input phasings, considering the shown choices in (*A*).

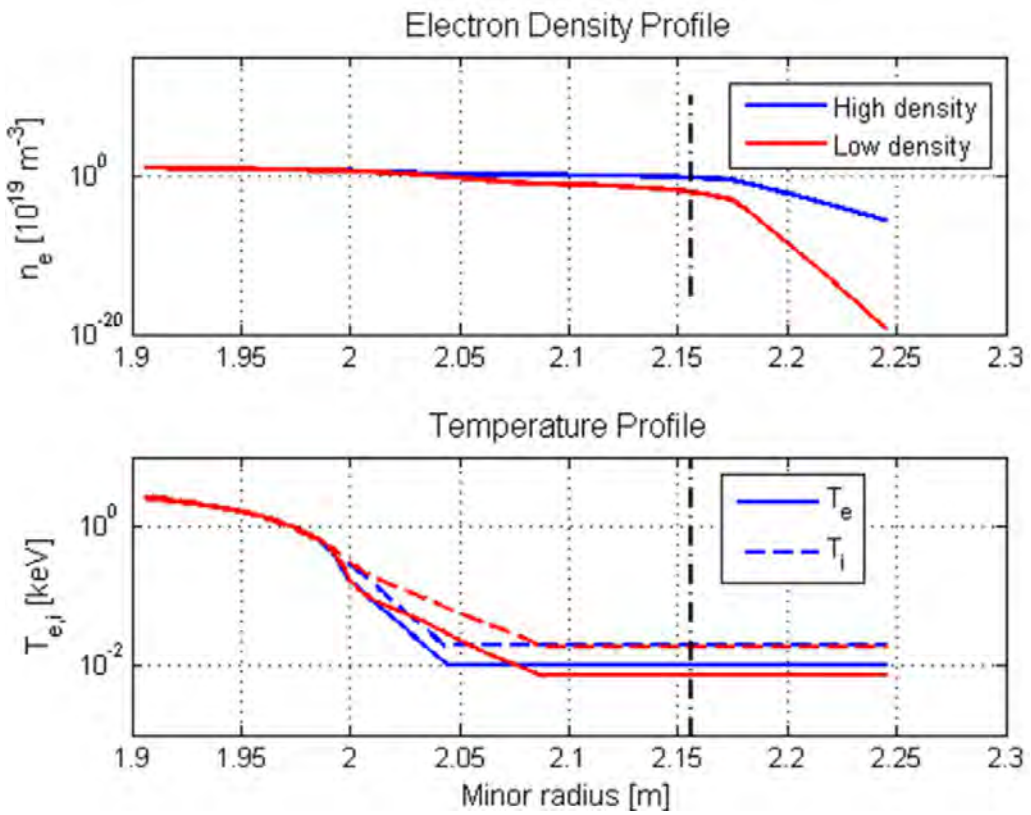

Figure 6. 2010 high (blue) and low (red) electron density profiles (top), ion (solid curve) and electron (dashed curve) temperature profiles (bottom).

toward the antenna were implemented for Case1 LO and Case2 LO profiles. In order to verify the effect of local gas puffing on the antenna performances, four cases were initially added, namely Case1 IPP, Case4 IPP, Case22 IPP and Case23 IPP (all 50% D and 50% T, 5.2 T). Afterwards, to further investigate gas puffing, additional 19 profiles were included during 2021;

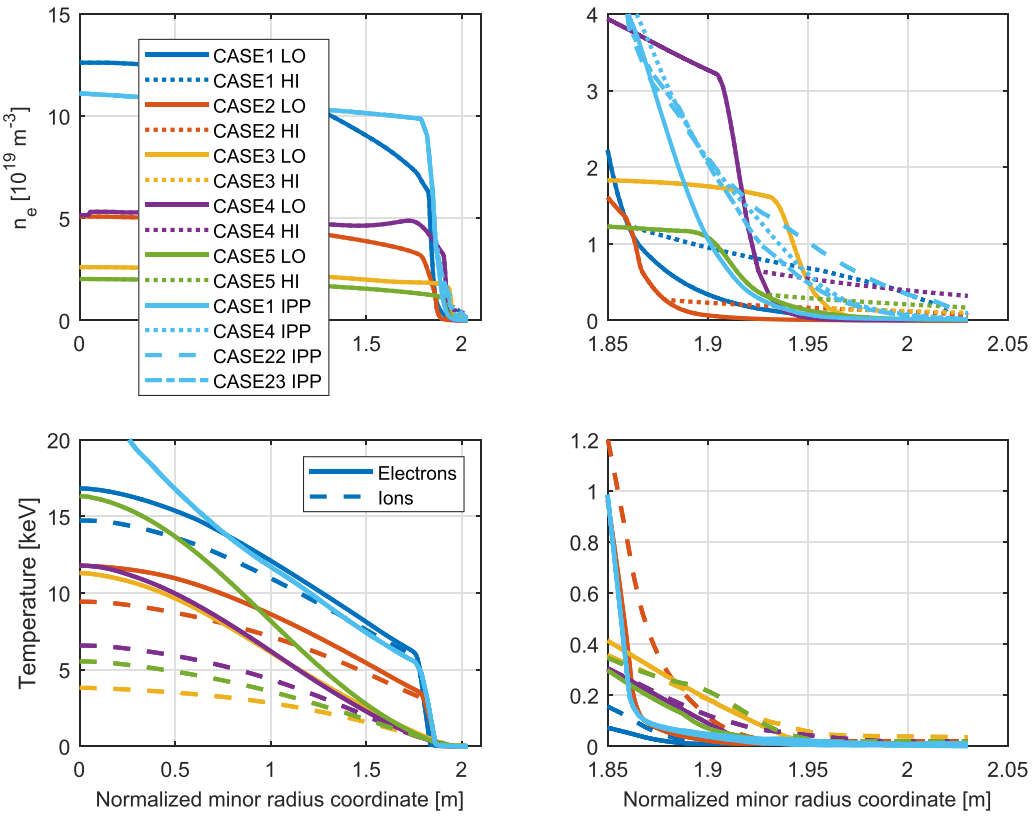

Figure 7. 2020 plasma profiles. Electron density is displayed on top, while ion and electron temperature are shown below; for both plots a zoomed view of the region in front of the antenna is shown on the right.

these last cases were simulated only for 'CY10' geometry at 55 MHz. Figure 7 displays all 2020 profiles.

2. Preliminary tests

2.1. Mesh sensitivity

The influence of the mesh resolution on the antenna aperture was first tested; geometry 'CY9a' (see section 1.2 for further details) was used as reference, keeping constant all geometrical features and the mesh resolution on conductors, and changing only the size of the mesh cells at the interface with plasma.

In general, TOPICA formulation requires that all the antenna's surfaces are discretized by means of triangular facets; the problem unknowns are then defined over couples of adjacent triangles. The size of the mesh on conductors is always below a user-defined threshold, usually less than 10 cm, but it can get really small depending on the geometrical details of the antenna. Mesh is finer, down to millimeters in size, on the antenna front part, while it is coarser on the back. The experience gained with several validation campaigns (for instance [15] or [16]) allowed to define the mesh on antenna metallic parts.

The mesh on the aperture is rather uniform instead, with triangles of approximately the same size. As already mentioned, the maximum number of unknowns on the aperture is bounded by the memory per node available on the computing cluster and, hence, cannot be raised at will. Four different cases were simulated at 47.5 MHz, loading both the low density 2010 profile and its 4 cm radial shift toward the launcher; table 2 shows the number of elements and their size for the four mesh cases.

The influence of the mesh resolution on the aperture was analyzed in terms of antenna input parameters, transferred power to plasma and radiated fields. In particular, the denser mesh case (Mesh 4 in table 2) was considered as a reference and the relative error with respect to that was computed. Figure 8 shows the effect on the antenna scattering parameters (only self terms are shown, being numerically the largest), both in magnitude and phase. It can be noted that the magnitude is only slightly influenced (error always below 1%), while the phase appears to be more sensitive to the mesh. Furthermore, the closer the plasma is to the antenna, the higher the relative error. If also off-diagonal terms are taken into account, the relative error rises for some entries to values above 100% for magnitude and above 400% for phase; this significant increase can be partly explained because off-diagonal elements of the scattering matrix are smaller (even two orders of magnitude) than the self terms.

A similar analysis was extended to the coupled power and to the maximum electric field in front of the FS, i.e. 1 cm from the aperture, once more considering the denser mesh geometry as the reference. Coupled power is computed assuming a simplified tuning and matching circuit, namely infinite coaxial lines connected to each port, with a maximum voltage

Table 2. Mesh resolution for the simulated cases.

	Mesh 1	Mesh 2	Mesh 3	Mesh 4
N. of triangles	1728	2688	3072	3456
N. of unknowns	2550	3980	4552	5124
Mesh min size on aperture	6.8 cm	5.5 cm	5.1 cm	4.9 cm
Mesh max size on aperture	9.8 cm	8.2 cm	7.4 cm	7.4 cm

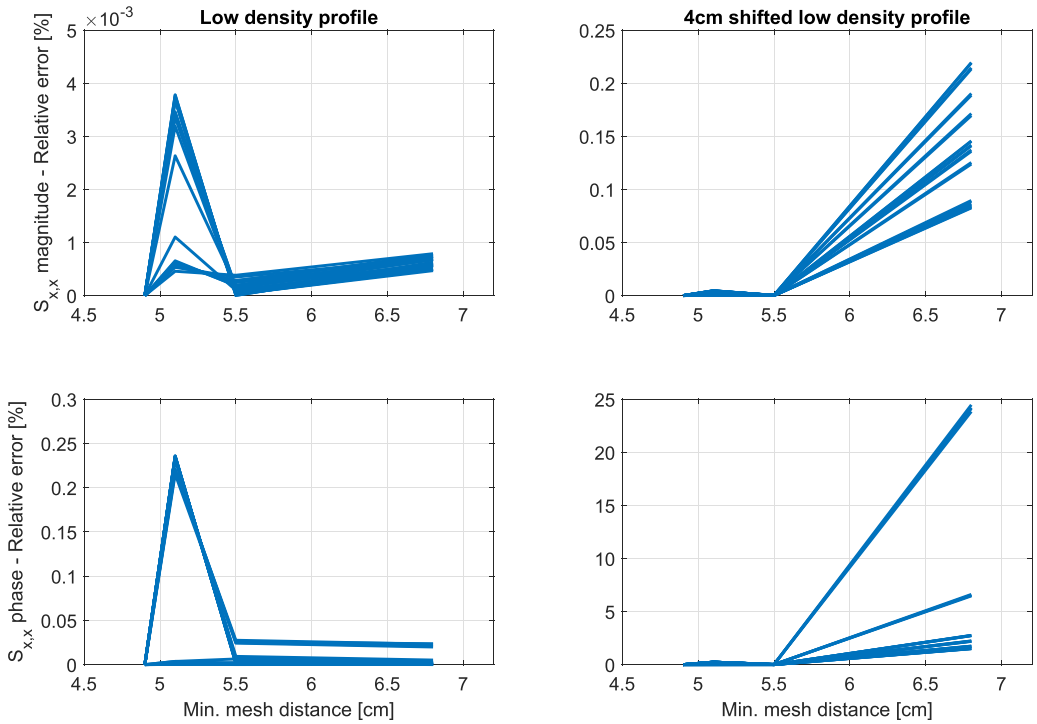

Figure 8. Relative error for the magnitude (top) and the phase (bottom) of the 24 self terms of the input scattering matrix, as a function of the minimum mesh size on the aperture. The low density profile is shown on the left, while the 4 cm shift is taken into account on the right. The denser mesh case, corresponding to 4.9 cm of minimum distance between mesh nodes, is used to normalize the relative error. Please notice that the error scale is considerably different for the two plasma cases.

of 45 kV. The electric field is evaluated imposing a magnitude of 1 V at each port with different phasings. Figure 9 documents again a substantial difference of the results in case of the coarser mesh for the 4 cm shifted low density plasma.

This test allowed to identify the mesh resolution necessary to get converged results. While a denser mesh is not strictly necessary, a coarser mesh can certainly lead to quite significant errors, above all in case of good coupling. In particular, the closer is the plasma to the antenna, the more evident is the influence of the mesh on the aperture.

2.2. FS impact

Geometry 'CY9' was again adopted to test the impact of the FS. To be more specific, the same launcher was simulated without FS at all ('CY9b'), with a simplified version of it ('CY9a') and with a much more detailed one ('CY9c'). Figure 2 allows us to visualize the difference between the two FS models. The 2010 low density profile and its 4 cm radial shift toward the antenna have been adopted for TOPICA computations at 40, 47.5 and 55 MHz. Performances over frequency have been estimated assuming a vacuum transmission line RF layout for an optimized excitation: the forward voltage waves at the launcher ports are such that the maximum voltages in the main transmission line (MTL) are equal with the phase of the MTL voltages at the average location of the voltage maxima corresponding to the requested phases and that the maximum voltage anywhere does not exceed 45 kV. Figure 10 shows for the different geometries the power coupled per launcher (neglecting losses) for both plasma loadings, assuming $0\pi0\pi$ toroidal and $0-\pi/2$ poloidal phasing for a maximum system voltage of 45 kV for both excitations.

As the reader can notice the influence of the FS model in terms of coupled power is rather small and approximately constant with frequency. The difference is larger when the FS is completely neglected. Conversely, the FS geometry has a substantial impact on the number of unknowns, as can be inferred by table 1; the simulation time is also roughly going as the square of the total number of unknowns. This motivated the usage of a simplified FS for the next set of simulations.

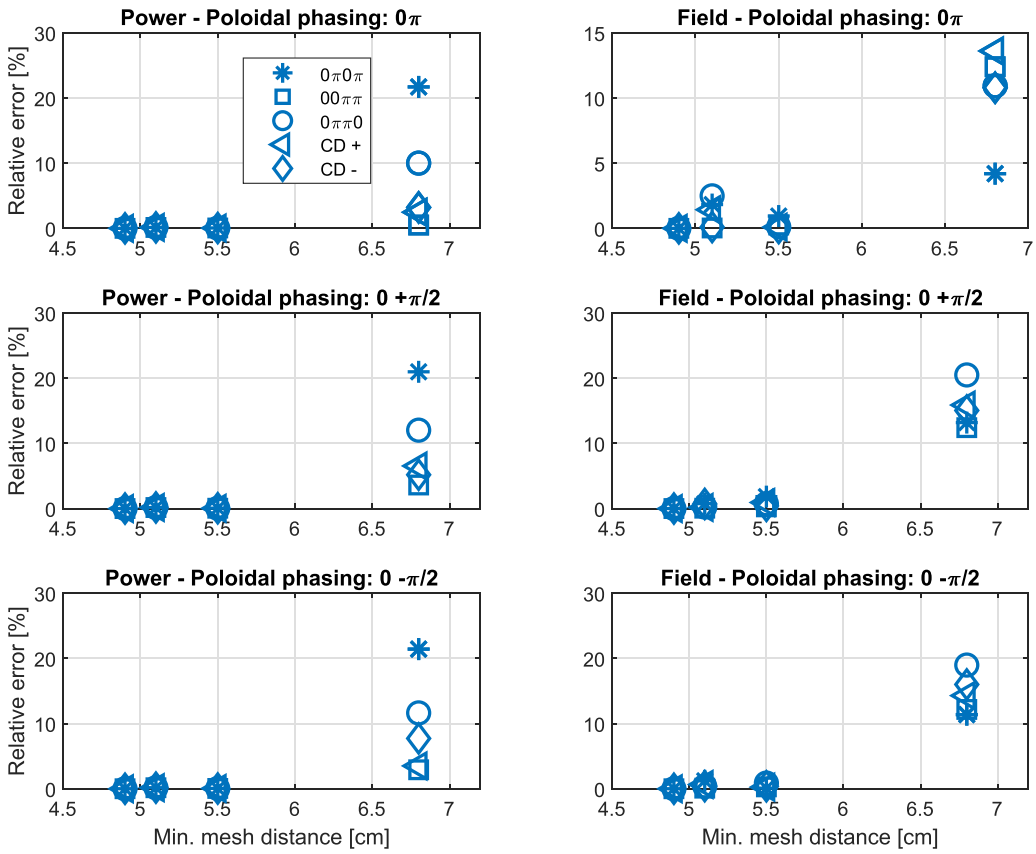

Figure 9. Relative error for the power coupled to plasma (left) and for the maximum electric field (right) for the 4 cm shifted low density plasma, as a function of the minimum mesh size on the aperture. Several toroidal and poloidal phasings are taken into account. The denser mesh case, corresponding to 4.9 cm of minimum distance between mesh nodes, is used to normalize the relative error.

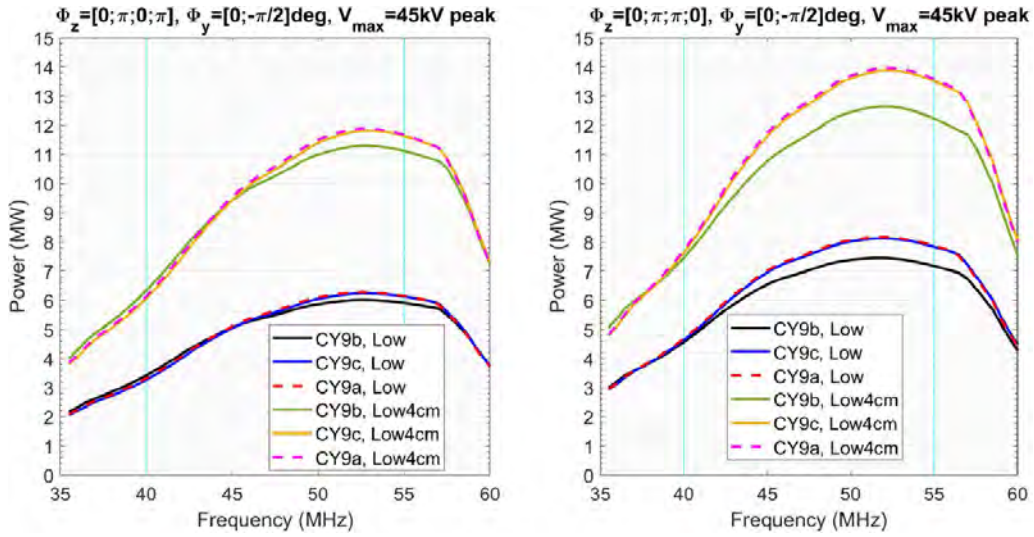

Figure 10. Estimated power coupled per launcher (neglecting losses) for the 2010 low density case and for its 4 cm shift toward the antenna. Two toroidal phasings are taken into account, namely $0\pi0\pi$ (left) and $0\pi\pi0$ (right), with constant poloidal phasing set to $0 - \frac{\pi}{2}$. The geometries without FS ('CY9b'), with simplified FS ('CY9a') and with realistic FS ('CY9c') are compared.

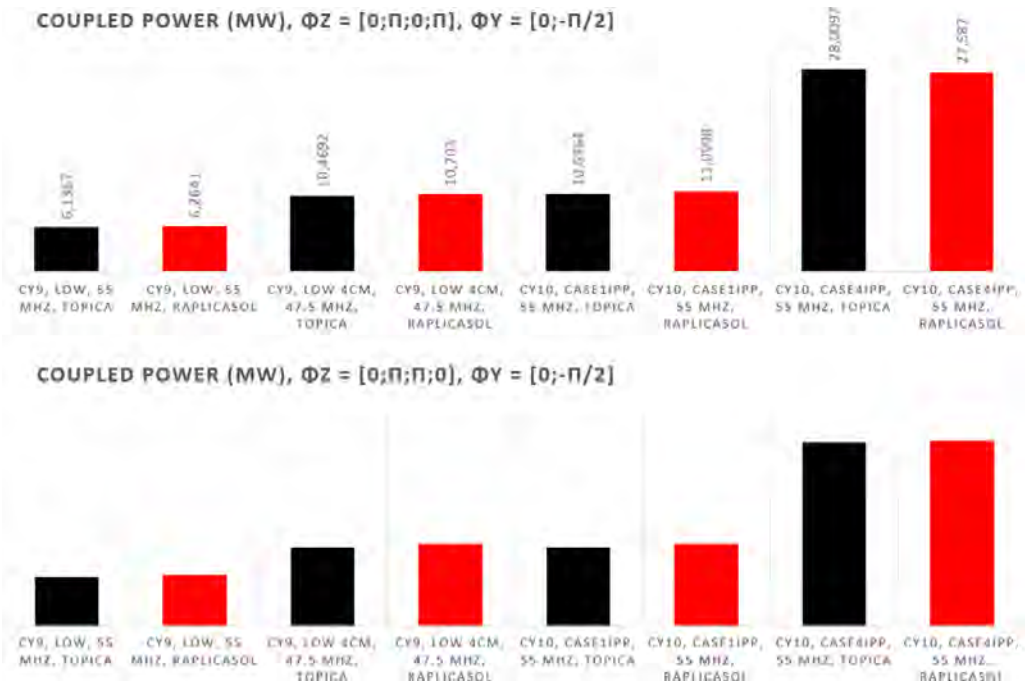

Figure 11. Comparison between the estimated power coupled per launcher (neglecting losses) by TOPICA (in black) and RAPLICASOL (in red) for two geometries ('CY9a' on the left, 'CY10' on the right) for a subset of plasma loadings at different frequencies, with constant poloidal phasing set to $0 - \frac{\pi}{2}$ and with $0\pi 0\pi$ (top) and $0\pi\pi 0$ (bottom) toroidal phasing.

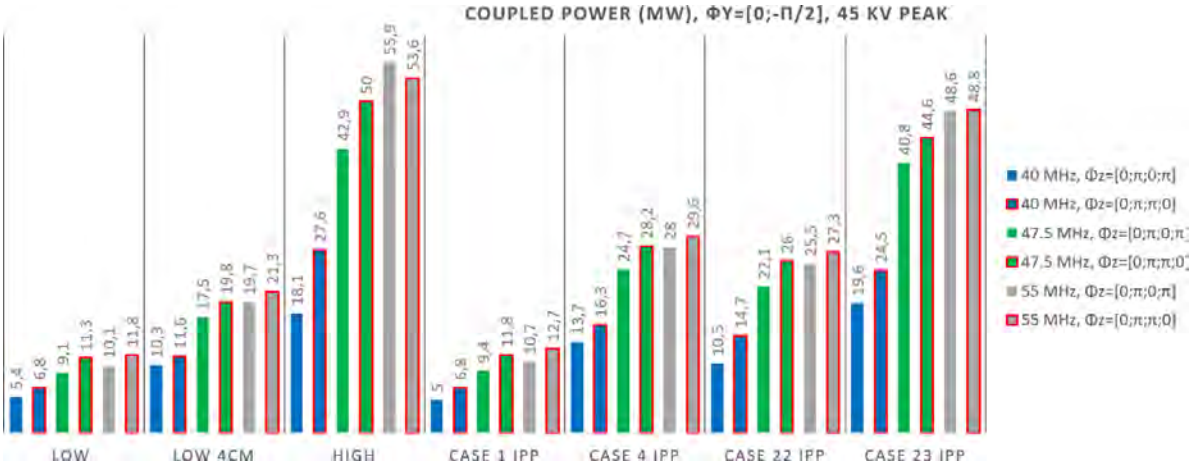

Figure 12. Estimated power coupled per launcher (neglecting losses) for the 'CY10' reference ITER IC antenna, for a subset of plasma loadings, with constant poloidal phasing set to $0 - \frac{\pi}{2}$ and varying toroidal phasing.

2.3. Benchmark with RAPLICASOL

TOPICA predictions were also bench-marked with a COMSOL-based RF code, namely RAPLICASOL [17], on both 'CY9a' and 'CY10' geometries, for a number of plasma cases, frequency points and input phasings. Figure 11 shows that there is on overall a very good agreement between the two coupling codes, with discrepancies that are below 5% for the runs under analysis. A specific paper is being prepared about all TOPICA-RAPLICASOL comparisons and for the additional modeling efforts.

3. Final geometry

Geometry 'CY10' is the current reference IO launcher for ITER. As outlined in section 1.2, it is a top-bottom asymmetrical antenna with a simplified FS structure and a few blanket tiles, as shown in figure 3. This launcher has been tested on five frequency points between 40 and 55 MHz, with all plasma profiles described in section 1.3, hence providing a very detailed overview of its performance. Figure 12 shows the power coupled to plasma for a single launcher for different working frequencies, input phasings and plasma loadings.

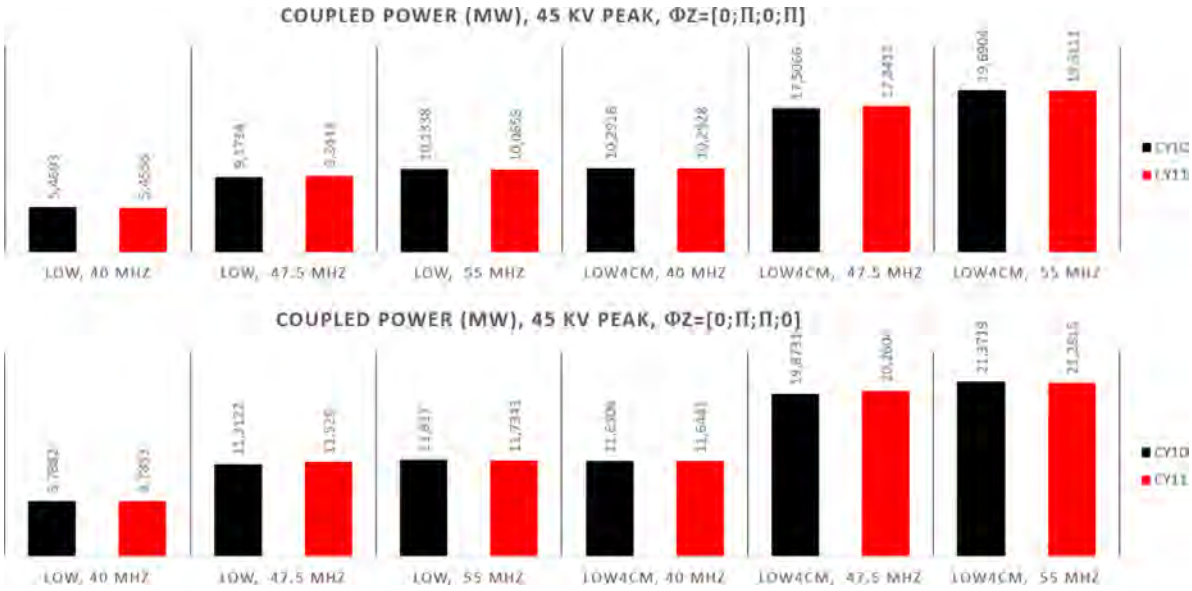

Figure 13. Estimated power coupled per launcher (neglecting losses) for the 'CY11' geometry (in red) and for the reference 'CY10' launcher (in black), for a subset of plasma loadings, with constant poloidal phasing set to $0 - \frac{\pi}{2}$ and with $0\pi0\pi$ (top) and $0\pi\pi0$ (bottom) toroidal phasing.

A total amount of 100 k cores hours has been used to complete all runs.

A more detailed description of the launcher and its performances will be available in a devoted paper. Similarly, this paper will also detail the comparison between geometries 'CY8', 'CY9' and 'CY10'.

3.1. Four-port junction

A last geometry based on the final launcher described in section 3 with the addition of the 4PJ has been also simulated with TOPICA, namely 'CY11'. This set of outputs was afterwards compared with the previous geometry where the 4PJ was simulated with a different commercial software (Ansys HFSS) and then added by means of its scattering parameters. Figure 13 documents the comparison, proving that the two different approaches (separate evaluation of the antenna front face and of the 4PJ behavior vs. simulation of the full system) are equivalent in terms of coupled power estimation.

4. Conclusions

A detailed analysis of the current ITER IC launcher with TOPICA code has been presented. Throughout the entire design task several large and complex geometries have been simulated with TOPICA, achieving an unprecedented level of detail and geometrical accuracy. Section 2.1 provides evidence that the S-matrix and coupled power are converged at the mesh resolution that we chose on the aperture; this is also confirmed by the comparison with RAPLICASOL presented in section 2.3, proving once more that TOPICA is a robust tool, which allows us to assist the design of ICRF antennas and assess their performances. Section 2.2 demonstrated that the FS should always be considered in the model but one can simplify the fine details, since they have a modest influence on the antenna performances (unless one would like to capture with precision the electric fields at the FS itself). Section 3.1 showed that a hybrid circuit/full-wave modeling (i.e. antenna portioned in a proper fashion to sub-components full-wave modeled separately and then combined together in RF circuit modeling) can be adopted to optimize the antenna with reduced numerical resources and faster simulation times instead of a full-wave modeling of the complete launcher (i.e. with the straps and 4PJs in a single full-wave simulation), without losing information with respect to the full array performance.

Acknowledgments

This work has been conducted under Contracts IO/20/CT/4300002118, IO/20/CT/4300002150 and IO/20/CT/4300002178. The views and opinions expressed herein do not necessarily reflect those of the ITER Organization. The authors would also like to thank A Loarte, M Schneider and F Köchl for the profiles generation and F Calarco for supervising the ITER ICRF antennas.

ORCID iDs

D. Milanesio https://orcid.org/0000-0002-5114-7235
A. Messiaen https://orcid.org/0000-0001-6537-1628
W. Tierens https://orcid.org/0000-0002-6979-8140
W. Zhang https://orcid.org/0000-0002-5951-6779

References

[1] Garcia-Regana J.M. and Okano K. 1999 *Nucl. Fusion* **39** 2495

[2] Tierens W. IPP-Garching/IO contract IO/20/CT/4300002150, Deliverable 8 *Assessments of the computational capabilities of COMSOL modelling* ITER_D_3TKBZ8 v3.2

[3] Tierens W. IPP-Garching/IO contract IO/20/CT/4300002150, Deliverable 9 *RAPLICASOL modelling of the ITER ICRF antenna* ITER_D_3TKJKF v3.0

[4] Bertelli N. *et al* Benchmark between antenna code TOPICA, RAPLICASOL and Petra-M for the ICRH ITER antenna *24th Topical Conf. on Radio-Frequency Power in Plasmas* submitted

[5] Bobkov V. *et al* Multi-strap ICRF antenna modeling and development in support of ITER and EU-DEMO *24th Topical Conf. on Radio-Frequency Power in Plasmas* submitted

[6] Louche F. *et al* Modal analysis of the fields in the ITER ICRF antenna port plug cavity *24th Topical Conf. on Radio-Frequency Power in Plasmas* submitted

[7] Lancellotti V., Milanesio D., Maggiora R., Vecchi G. and Kyrytsya V. 2006 *Nucl. Fusion* **46** S476–99

[8] Milanesio D., Meneghini O., Lancellotti V., Maggiora R. and Vecchi G. 2009 *Nucl. Fusion* **49** 115019

[9] Brambilla M. 1993 *Plasma Phys. Control. Fusion* **35** 41–62

[10] Milanesio D. and Maggiora R. 2010 *Nucl. Fusion* **50** 025007

[11] Messiaen A., Koch R., Weynants R.R., Dumortier P., Louche F., Maggiora R. and Milanesio D. 2010 *Nucl. Fusion* **50** 025026

[12] Stix T.H. 1992 *Waves in Plasmas* (American Institute of Physics)

[13] Loarte A. 2008 private communication

[14] Lamalle P. 2020 *Technical Report* ITER_D_23G78Q v1.1

[15] Milanesio D., Lancellotti V., Colas L., Maggiora R., Vecchi G. and Kyrytsya V. 2007 *Plasma Phys. Control. Fusion* **49** 405–19

[16] Stepanov I. *et Al* 2015 *Nucl. Fusion* **55** 113003

[17] Tierens W. *et al* 2019 *Nucl. Fusion* **59** 046001